ACS APPLIED MATERIALS & INTERFACES

Research Article

www.acsami.org

Tailoring Oxygen Sensitivity with Halide Substitution in Difluoroboron Dibenzoylmethane Polylactide Materials

Christopher A. DeRosa, Caroline Kerr, Ziyi Fan, Milena Kolpaczynska, Alexander S. Mathew, Ruffin E. Evans, Guoqing Zhang, and Cassandra L. Fraser*

Department of Chemistry, University of Virginia, Charlottesville, Virginia 22904, United States

Supporting Information

ABSTRACT: The dual-emissive properties of solid-state difluoroboron β-diketonate-poly(lactic acid) (BF_2bdkPLA) materials have been utilized for biological oxygen sensing. In this work, BF_2dbm(X)PLA materials were synthesized, where X = H, F, Cl, Br, and I. The effects of changing the halide substituent and PLA polymer chain length on the optical properties in dilute CH_2Cl_2 solutions and solid-state polymer films were studied. These luminescent materials show fluorescence, phosphorescence, and lifetime tunability on the basis of molecular weight, as well as lifetime modulation via the halide substituent. Short BF_2dbm(Br)PLA (6.0 kDa) and both short and long BF_2dbm(I)PLA polymers (6.0 or 20.3 kDa) have fluorescence and intense phosphorescence ideal for ratiometric oxygen sensing. The lighter halide-dye polymers with hydrogen, fluorine, and chlorine substitution have longer phosphorescence lifetimes and can be utilized as ultrasensitive oxygen sensors. Photostability was also analyzed for the polymer films.

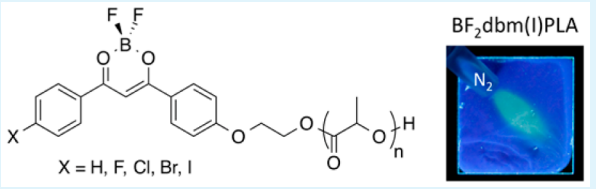

KEYWORDS: *difluoroboron β-diketonate complexes, room-temperature phosphorescence, heavy atom effect, poly(lactic acid), photostability*

INTRODUCTION

Developing luminescent materials for *in vivo* biological research can be a daunting task.[1−3] Brightness and biocompatibility are prerequisites. Dyes must be capable of reporting the concentration of an analyte over a biologically relevant range while retaining essential photophysical properties.[4,5] Difluoroboron-based fluorophores, such as 4,4-difluoro-4-bora-3a,4a-diaza-*s*-indacenes (BODIPY), are common fluorescent reporters, because they satisfy these conditions.[6,7] Other difluoroboron fluorophores, including β-diketonates (OBO),[8] β-diiminates (NBN),[9,10] and β-ketoiminates (OBN),[11,12] have also been utilized for their unique structural and optical properties. A distinguishing feature of the difluoroboron β-diketonate dyes is that the fluorescence is bright in both solution and the solid state, making them ideal for liquid crystals,[13,14] ion indicators,[15] and mechanochromic materials.[16,17]

Difluoroboron β-diketonate (BF_2bdk) dyes, combined with poly(lactic acid) (PLA), exhibit short-lived fluorescence and long-lived phosphorescence at room and body temperatures.[18−20] Thus, these dye-PLA conjugates can serve as single-component ratiometric oxygen sensors without the need for fluorophore/phosphor/matrix mixtures. Fluorescence serves as an internal standard while phosphorescence, which is susceptible to oxygen quenching, serves as the sensor.[21−23] As the dyes are exposed to oxygen, the fluorescence-to-phosphorescence (F/P) intensity ratio is measured and compared to an oxygen calibration curve to determine the concentration of oxygen present. In addition to fostering dual emissive properties of BF_2bdk dyes—fluorescence and phosphorescence, rather than just fluorescence alone—PLA is a good choice because it is a biocompatible and degradable polymer.[24,25] Furthermore, processing is well-established.[26,27] For example, boron nanoparticles (BNPs) can be produced from these dye−PLA conjugates, serving as useful tools in biomedical imaging applications.[26]

It is widely known that halide substituents can modulate structural and optical properties of materials. Previously, Baronoff et al. showed that halide substitution of cyclometalled iridium complexes can alter the ligand geometry and band-gap properties.[28] In addition, Kim et al. recently presented benzaldehyde/dibromobenzene co-crystals with tunable phosphorescence by changing alkyl chain length and halide substitution.[29,30] Mechanochromic luminescence (ML)[31] and mechanochromic luminescence quenching (MLQ) have also been reported with halide-substituted BF_2dbm(X)$C_{12}H_{25}$ materials, where X = F, Cl, Br, I.[32] Previously reported difluoroboron dibenzoylmethane polylactide (BF_2dbmPLA) materials (Figure 1, X = H) had phosphorescence lifetimes in the range of a hundred milliseconds (80−150 ms), depending on the polymer molecular weight,[19] while the iodine-substituted derivatives (BF_2dbm(I)PLA) had phosphorescence lifetimes of only 4−5 ms.[22] This change in heavy atom substitution drastically affected the oxygen sensitivity of these materials. The BF_2dbmPLA materials are highly sensitive in the

Received: August 4, 2015
Accepted: September 28, 2015
Published: October 19, 2015

DOI: 10.1021/acsami.5b07126
ACS Appl. Mater. Interfaces 2015, 7, 23633−23643

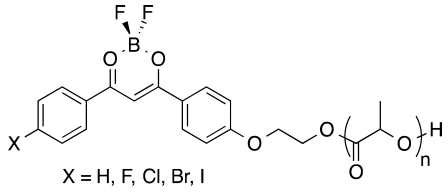

Figure 1. Difluoroboron dibenzoylmethane–poly(lactic acid) and halide-substituted derivatives.

hypoxic range (0–1% O_2), while BF_2dbm(I)PLA can effectively sense up to ambient conditions (0–21% O_2). Dyes with different oxygen sensitivities can be adapted for various biological applications.[33] For example, probes with high sensitivities within 0.5–3.0% O_2 are well-suited for tumor hypoxia imaging,[34,35] and probes with a sensitivity of 2%–6% O_2 can monitor brain oxygenation in great detail,[36] while less-sensitive probes (with sensitivities within the O_2 range of 5%–15%) can effectively monitor blood oxygenation (veins versus arteries).[37]

Here, a systematic study of the effects of halide substitution on BF_2dbmPLA optical and oxygen sensing properties is reported. A series of halide-substituted BF_2dbm(X)PLA materials were synthesized, where X = H, F, Cl, Br, and I (Figure 1), to effectively tune the triplet emission of the materials via an internal electron withdrawing group and heavy atom effects. Dye–polymer conjugates can be fabricated into nanoparticles[26] or nanofibers[27] for biomedical imaging, minimizing phase separation, heterogeneity and dye leaching that can occur for comparable dye loadings in dye/PLA blends. The dyes and polymers are analyzed in dilute CH_2Cl_2 solutions and in solid-state films. In the solid state, phosphorescence lifetime, and thus oxygen sensitivity, can be controlled with the halide substituent and polymer molecular weight. The photostability of the polymers was studied over extended excitation times (~18 h) with a hand-held UV light source.

MATERIALS AND METHODS

3,6-Dimethyl-1,4-dioxane-2,5-dione (D,L-lactide, Sigma–Aldrich) was recrystallized twice from ethyl acetate and stored under nitrogen. The ligand precursor 1-(4-(2-((tetrahydro-2H-pyran-2-yl)oxy)ethoxy)-phenyl)ethan-1-one[38] ligands dbmOH (**1**)[18] and dbm(I)OH (**5**),[22] boron initiators BF_2dbmOH (**6**)[18] and BF_2dbm(I)OH (**9**)[22] and polymers **11**–**15**[23] were prepared as previously described. Tin(II) 2-ethylhexanoate ($Sn(oct)_2$, Spectrum), boron trifluoride diethyl etherate (Aldrich, purified, redistilled), and all other reagents and solvents were used as received, without further purification. Solvents CH_2Cl_2 and THF were dried and purified over 3 Å molecular sieves activated at 300 °C.[39] All other chemicals were reagent-grade from Sigma–Aldrich and were used without further purification.

^{1}H NMR spectra were recorded on a Varian Unity Inova 300/51 (300 MHz) or a Varian VMRS/600 (600 MHz) instrument in $CDCl_3$. ^{1}H NMR peaks were referenced to the signals for the residual protiochloroform at 7.26 ppm. Coupling constants are given in units of Hertz. Polymer molecular weights were determined by gel permeation chromatography (GPC) (tetrahydrofuran (THF), 25 °C, 1.0 mL/min, d*n*/d*c* = 0.050) using multiangle laser light scattering (SEC-MALS) (λ = 658 nm, 25 °C) and refractive index (RI) (λ = 658 nm, 25 °C) detection. Polymer Laboratories 5 μm mixed-C columns (guard column plus two columns), along with various instrumentation (Wyatt Technology, Model Optilab T-rEX interferometric refractometer, miniDAWN TREOS multiangle static light scattering (MALS) detector, ASTRA 6.0 software, and Agilent Technologies, Series 1260 HPLC with diode array (DAD) detector, ChemStation) were used in GPC analysis. Polymer characterization data is provided in the Supporting Information (Figures S7–S16) and Table 1 (presented later in this work). UV–vis spectra were recorded on a Hewlett-Packard Model 8452A diode-array spectrophotometer.

Luminescence Measurements. Steady-state fluorescence emission spectra were recorded on a Horiba Fluorolog-3 Model FL3-22 spectrofluorometer (double-grating excitation and double-grating emission monochromator). A 2 ms delay was used when recording the delayed emission spectra. Time-correlated single-photon counting (TCSPC) fluorescence lifetime measurements were performed with a NanoLED-370 (λ_{ex} = 369 nm) excitation source and a DataStation Hub as the SPC controller. Phosphorescence lifetimes were measured with a 1 ms multichannel scalar (MCS) excited with a flash xenon lamp (λ_{ex} = 369 nm; duration <1 ms). Lifetime data were analyzed with DataStation v2.4 software from Horiba Jobin Yvon. Fluorescence quantum yields (Φ_F) of initiator and polymer samples in CH_2Cl_2 were calculated against anthracene as a standard, as previously described, using the following values: Φ_F (anthracene) = 0.27[40,41], n_D^{20} (EtOH) = 1.360, n_D^{20} (CH_2Cl_2) = 1.424.[42] Optically dilute CH_2Cl_2 solutions of the dyes, with absorbances of <0.1 a.u., were prepared in 1-cm-path-length quartz cuvettes. Thin films were prepared on the inner wall of vials by dissolving polymers in CH_2Cl_2 (2 mg/mL) and evaporating the solvent by slowly rotating the vial under a low stream of nitrogen. The solution-cast films were then dried *in vacuo* for at least 15 min before measurements. Fluorescence spectra and lifetimes were obtained under ambient conditions (e.g., air, ~21% oxygen). Phosphorescence measurements were performed under a N_2 atmosphere. The vials with the solution-cast films were purged and sealed with a Teflon cap and wrapped in parafilm in a glovebox prior to measurements. The glovebox was purged for 30 min prior to samples being sealed. For oxygen sensitivity measurements, solution-cast films in vials were fitted with a 12 mm PTFE/silicone/PTFE seal (Chromatography Research Supplies), connected by a screw cap. Vials were continuously purged with analytical-grade N_2 (Praxair) or 1.0% O_2 (Praxair) during measurements. For 21% O_2 (i.e., air), measurements were taken under ambient conditions (open vial, no cap). Fluorescence and phosphorescence lifetimes were fit to double or triple exponential decays in solid-state films.

Photostablility Measurements. Spin-cast films were prepared by dropwise addition of 1 mL of a ~1.0 mg/mg CH_2Cl_2 solution on 18 mm × 18 mm glass cover slides (Fisher Scientific) using a Laurel Technologies WS-650s spin-coater at 3000 rpm. Films were dried *in vacuo* for ~15 min prior to measurements. Films were placed on a black surface 10 cm below the camera and were irradiated with a 4 W UV lamp. A Watec 902H2 Ultimate monochrome CCD camera, equipped with a Fujinon DV5 × 3.6R4B-SA2L 3.6–18 mm F/1.8 lens and an Ion Video 2 PC analog-to-digital converter was used to monitor photostability. Linearity was ensured by a neutral density filter calibration (Tiffen, 58 mm Neutral Density = 0.9) and by disabling automatic gain and gamma control. A custom-made MATLAB program was implemented to record the pixel intensity of each sample every 5 min for 18 h.

*1-(4-Fluorophenyl)-3-(4-(2-hydroxyethoxy)phenyl)propane-1,3-dione (dbm(F)OH) (**2**).* The aromatic ketone, 1-(4-(2-((tetrahydro-2H-pyran-2-yl)oxy)ethoxy)phenyl)ethan-1-one[38] (870 mg, 3.3 mmol), and ethyl 4-fluorobenzoate (674 mg, 3.9 mmol), were dissolved in anhydrous THF (50 mL). A suspension of NaH (120 mg, 5.0 mmol) in THF (10 mL) was transferred to the reaction via cannula. The reaction was refluxed at 60 °C under a nitrogen atmosphere, and monitored by TLC, until consumption of the aromatic ketone was complete (7 h). The reaction mixture was removed from the heat and allowed to cool to room temperature (RT), before excess NaH was quenched with saturated aqueous $NaHCO_2$ (20 mL), and the THF was removed via rotary evaporation. The crude reaction mixture was treated with 1 M HCl to adjust the pH to ~5. The resulting mixture was extracted with EtOAc (2 × 20 mL), then combined organic layers were washed with H_2O (2 × 20 mL). The organic solvent, EtOAc, was removed via rotary evaporation to yield a brown oil. The crude reaction mixture was dissolved in a THF (100 mL)/H_2O (20 mL) solution, a catalytic amount of TsOH (20 mg, 0.12 mmol) was added, and then the reaction mixture was refluxed at 60 °C and monitored by

DOI: 10.1021/acsami.5b07126
ACS Appl. Mater. Interfaces 2015, 7, 23633–23643

TLC for the disappearance of protected diketone (2 h). The THF was removed by rotary evaporation, resulting in an aqueous suspension of the crude organic product. The organics were extracted with CH_2Cl_2 (2 × 20 mL), washed with H_2O (2 × 20 mL) and brine (2 × 20 mL), and dried over anhydrous Na_2SO_4. The mixture was filtered and the solvent was removed by rotary evaporation to yield a brown solid. The crude solid was purified by recrystallization (EtOAc/hexanes) to yield a white powder: 649 mg (65%). ^{1}H NMR (600 MHz, $CDCl_3$): δ 17.10 (s, broad, 1H, −OH), 8.03−7.93 (m, broad, 4 H, 2′, 6′-Ar*H*, 2″, 6″-Ar*H*), 7.20−7.10 (m, broad, 2H, 3′, 5′-Ar*H*), 6.99 (d, J = 9, 2H, 3″,5″-Ar*H*), 6.74 (s, 1H, −COC*H*CO), 4.17 (t, J = 6, 2H, Ar-OCH_2CH$_2$OH), 4.01 (t, J = 6, 2H, Ar−OCH$_2$CH_2OH), 1.65 (s, broad, 1H, Ar−OCH$_2$CH$_2$O*H*). HRMS (ESI, TOF) m/z calcd for $C_{17}H_{16}O_4F$, 303.1033 $[M + H]^+$; found 303.1031.

*1-(4-Chlorophenyl)-3-(4-(2-hydroxyethoxy)phenyl)propane-1,3-dione (dbm(Cl)OH) (**3**).* The chloro ligand (**3**) was prepared as described for **2**, but methyl 4-chlorobenzoate was used as the aromatic ester in the Claisen condensation to yield a tan flaky solid: 210 mg (45%). ^{1}H NMR (300 MHz, $CDCl_3$): δ 16.91 (s, broad, 1H, −OH), 7.96 (d, J = 9, 2H, 2′, 6′-Ar*H*), 7.89 (d, J = 8.4, 2H, 2″,6″-Ar*H*), 7.44 (d, J = 8.4, 2H, 3′,5′-Ar*H*), 7.00 (d, J = 9, 2H, 3″,5″-Ar*H*), 6.74 (s, 1H, −COC*H*CO−), 4.16 (t, J = 4.2, 2H, −ArOCH_2−), 4.00 (s, broad, 2H, −CH_2OH), 3.50 (s, broad, 1H, −CH$_2$O*H*). HRMS (ESI, TOF) m/z calcd for $C_{17}H_{16}O_4Cl$ 319.0728 $[M + H]^+$; found 319.0737.

*1-(4-Bromophenyl)-3-(4-(2-hydroxyethoxy)phenyl)propane-1,3-dione (dbm(Br)OH) (**4**).* The bromo ligand (**4**) was prepared as described for **2**, but methyl 4-bromobenzoate was used as the aromatic ester in the Claisen condensation to yield a tan powder: 855 mg (63%). ^{1}H NMR (300 MHz, $CDCl_3$): δ 16.90 (s, broad, 1H, −OH), 7.97 (d, J = 9, 2H, 2′, 6′-Ar*H*), 7.83 (d, J = 8.4 2H, 2″,6″-Ar*H*), 7.62 (d, J = 8.4, 2H, 3′,5′-Ar*H*), 7.00 (d, J = 9, 2H, 3″,5″-Ar*H*), 6.75 (s, 1H, −COC*H*CO−), 3.89 (s, 3H, −ArOCH_3), 4.17 (t, J = 4.2, 2H, −ArOCH_2−), 4.02 (s, broad, 2H, −CH_2OH), 1.99 (s, broad, 1H, −CH$_2$O*H*). HRMS (ESI, TOF) m/z calcd for $C_{17}H_{16}O_4Br$ 363.0232 $[M + H]^+$; found 363.0237.

*BF$_2$dbm(F)OH (**7**).* The fluoro initiator **7** was prepared by dissolving dbm(F)OH (**2**) (200 mg, 0.66 mmol) in anhydrous CH_2Cl_2 (50 mL) in a dry 100 mL round-bottom flask. Boron trifluoride diethyl etherate (122 μL, 0.99 mmol) was added via syringe, whereupon the solution turned light yellow. The reaction mixture was stirred at room temperature and monitored by TLC until the ligand substrate was consumed (4 h). Excess boron trifluoride diethyl etherate was quenched by the addition of $K_2CO_{3\ (s)}$ (100 mg, 0.72 mmol). After stirring for 15 min, the reaction mixture was filtered and the solvent was removed via rotary evaporation to yield a dark yellow powder. The product was purified by column chromatography (1:1 hexanes/EtOAc, then EtOAc) to yield a faint yellow powder: 151 mg (69%). ^{1}H NMR (600 MHz, $CDCl_3$): δ 8.17−8.14 (m, broad, 4H, 2′,6′-Ar*H*, 2″,6″-Ar*H*), 7.21 (d, J = 6, 2H, 3′,5′-Ar*H*), 7.07−7.04 (m, 2H, 3″,5″-Ar*H*), 6.97 (s, 1H, COC*H*CO), 4.99 (s, 1H, Ar−OCH$_2$CH$_2$O*H*), 4.21 (t, J = 6, 2H, Ar−OCH_2CH$_2$OH), 4.03 (t, J = 6, 2H, Ar−OCH$_2$CH_2OH). HRMS (ESI, TOF) m/z calcd for $C_{17}H_{14}O_4BF_2$ 331.0953 $[M - F]^+$; found 331.0949.

*BF$_2$dbm(Cl)OH (**8**).* The chloro initiator **8** was prepared as described for **7**, using dbm(Cl)OH (**3**) instead of dbm(F)OH (**2**). A yellow powder was obtained: 118 mg (76%). ^{1}H NMR (600 MHz, $CDCl_3$): δ 8.16 (d, J = 9, 2H, 2′,6′-Ar*H*), 8.06 (d, J = 9, 2H, 2″,6″-Ar*H*), 7.52 (d, J = 8.4, 2H, 3′,5′-Ar*H*), 7.07−7.05 (m, 3H, 3″,5″-Ar*H*, −COC*H*CO−), 4.21 (t, J = 3.9, 2H, −ArOCH_2−), 4.04−4.02 (m, 2H, −CH_2OH). HRMS (ESI, TOF) m/z calcd for $C_{17}H_{14}O_4ClBF$ 347.0661 $[M - F]^+$; found 347.0658.

*BF$_2$dbm(Br)OH (**9**).* The bromo initiator was prepared as previously described for **7**, using dbm(Br)OH (**4**) instead of dbm(F)OH (**2**). A yellow powder was obtained: 110 mg (49%). ^{1}H NMR (600 MHz, $CDCl_3$): δ 8.16 (d, J = 9, 2H, 2′,6′-Ar*H*), 7.97 (d, J = 9, 2H, 2″,6″-Ar*H*), 7.69 (d, J = 8.4, 2H, 3′,5′-Ar*H*), 7.07−7.05 (m, 3H, 3″,5″-Ar*H*, −COC*H*CO−), 4.21 (t, J = 3.9, 2H, −ArOCH_2−), 4.07−4.03 (m, 2H, −CH_2OH). HRMS (ESI, TOF) m/z calcd for $C_{17}H_{14}O_4BrBF$ 391.0153 $[M - F]^+$; found 391.0156.

RESULTS AND DISCUSSION

Synthesis. The β-diketones **1**−**5** (Scheme 1) were prepared as previously described.[38] Namely, the aromatic ketone 1-(4-(2-((tetrahydro-2H-pyran-2-yl)oxy)ethoxy)phenyl)ethan-1-one was combined with the appropriate aromatic ester to generate the diketone via a Claisen condensation, followed by removal of the dihydropyran hydroxyl protecting group, to give compounds **1**−**5**. By varying the aromatic ester, ligands with different halide substituents were easily produced via the same synthetic methods. The diketones were purified by recrystallization in EtOAc and hexanes.

Scheme 1. Synthesis of Dye-PLA Conjugates

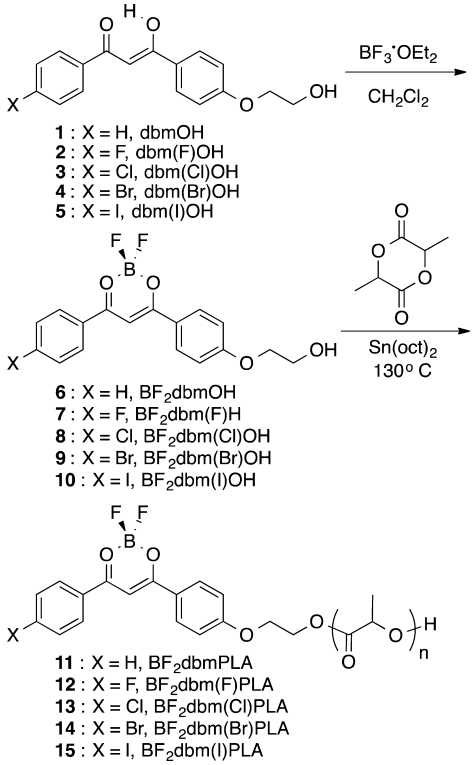

Boronation was performed by stirring boron trifluoride diethyl etherate with the β-diketones, **1**−**5**, in anhydrous CH_2Cl_2 for 4−10 h at room temperature. The parent compound, BF_2dbmOH (**6**), and the iodine-substituted BF_2dbm(I)OH (**10**) were purified by recrystallization from acetone/hexanes to obtain yellow crystalline powders. The lighter halide derivatives (**7**−**9**) had solubilities that were very similar to that of the ligand analogues and were instead purified by silica column chromatography (EtOAc/hexanes eluent) and also obtained as yellow powders.

Poly(lactic acid) (PLA) was grown from the primary alcohol sites of boron initiators **6**−**10** in lactide melts, in the presence of a stannous octoate catalyst, as previously described.[23] Compared to less-soluble dinaphthyl initiators,[23] **6**−**10** readily dissolved, even in low loadings of molten lactide (i.e., 50 equiv). To assess the effects of molecular weight (MW) on the luminescence properties of dye-PLA conjugates, two polymers were grown for each halide initiator—one with low MW (6.0−7.5 kDa) and one with higher MW (16.5−20.0 kDa) (see Table 1). With 50 equiv of lactide, polymerizations became viscous and were stopped after 1 h by cooling to room temperature, followed by precipitation from CH_2Cl_2/ice cold MeOH and

DOI: 10.1021/acsami.5b07126
ACS Appl. Mater. Interfaces 2015, 7, 23633−23643

Table 1. Polymer Molecular Weight Characterization

polymer	loading[a]	M_n (NMR)[b]	M_n (GPC)[c]	M_w (GPC)[c]	polydispersity index, PDI[c]
11a	50:1/40	6000	6600	6900	1.05
12a	50:1/40	6200	6100	6600	1.08
13a	50:1/40	7700	7500	8200	1.09
14a	50:1/40	5800	6400	7600	1.18
15a	50:1/40	6700	6600	7100	1.08
11b	200:1/40	24 200	19 100	20 800	1.09
12b	200:1/40	20 400	16 500	18 500	1.12
13b	200:1/40	23 400	18 700	20 600	1.10
14b	200:1/40	18 500	17 100	18 500	1.08
15b	200:1/40	24 200	20 300	23 100	1.14

[a]Molar ratio of monomer to $Sn(oct)_2$ catalyst per equiv boron initiator. [b]Molecular weights determined by end-group analysis (Dye-Ar-OCH_2CH_2– vs PLA-CH integration). [c]PDI = M_w/M_n, as determined by GPC.

then CH_2Cl_2/hexanes.[23] Reactions with 200 equiv were typically run for 3 h. Reactions were stopped at ∼60%–80% conversion to ensure more controlled reaction conditions and polymers with low polydispersities (1.05–1.18). This minimizes thermal depolymerization or transesterification side reactions, as previously described.[43,44]

Optical Properties in Solution. The dye initiators (**6**–**10**) and polymers (**11**–**15**) were analyzed in dilute CH_2Cl_2 solutions in air at room temperature; the optical properties are summarized in Table 2. The dyes and polymers have almost-identical properties in CH_2Cl_2 and all absorb light in the UV to violet range (395–410 nm; see Figure S17 in the Supporting Information). As the halide substituent becomes heavier, the absorbance is red-shifted (i.e., BF_2dbmOH (**6**) λ_{abs} = 397 nm versus BF_2dbm(I)OH (**10**) λ_{abs} = 407 nm). The extinction coefficient increased slightly with heavier halides as well (BF_2dbmOH (**6**) ε = 53 000 M^{-1} cm^{-1} versus BF_2dbm(I)OH (**10**) ε = 58 000 M^{-1} cm^{-1}). As is commonly observed,[18] extinction coefficients decreased from dyes to polymers with the same halide substituent (i.e., BF_2dbm(F)OH (**7**): ε = 48 000 M^{-1} cm^{-1} versus BF_2dbm(F)PLA (**12a**) ε = 45 000 M^{-1} cm^{-1}), perhaps due to minor dye degradation during the polymerization, purification processes, or inherent error in estimating dye content and ascribing an extinction coefficient to polydisperse samples.

The dyes emit blue fluorescence in CH_2Cl_2 solution, and the halide substituents have only minor influences on the color (BF_2dbmOH (**6**); λ_F = 433 nm, BF_2dbm(I)OH (**10**); λ_F = 441 nm). However, halide substitution does alter the fluorescence lifetime (τ_F) and quantum yield (Φ_F) of the boron dyes. Lighter halide dyes and polymers (X = H, F, Cl, and Br) have similar lifetimes of (∼1.95 ns), and quantum yields near unity (∼0.95). The iodine derivatives showed lower quantum yields and shorter fluorescence lifetimes, as a result of the heavy atom effect.[22] In solution, enhanced intersystem crossing via the heavy atom effect resulted in nonradiative decay pathways, as a result of oxygen quenching or intramolecular motions.

Optical Properties of Films. Boron polymers were also studied as films in the solid state. Optical properties for polymers **11**–**15** with variable molecular weights are presented in Table 3. Fluorescence spectra and lifetime measurements were obtained under ambient conditions (e.g., air, ∼21% oxygen). Phosphorescence measurements were conducted under N_2.

Table 3. Optical Properties of Solution-Cast Films

			Fluorescence		Phosphorescence	
sample		M_n[a] (kDa)	λ_{em}[b] (nm)	τ_{pw0}[c] (ns)	λ_{em}[d] (nm)	τ_{pw0}[e] (ms)
BF_2dbmPLA	**11a**	6.6	457	6.63	516	142.1
	11b	19.1	426	1.53	510	207.4
BF_2dbm(F)PLA	**12a**	6.1	502	45.47	512	122.8
	12b	16.5	428	2.53	508	195.9
BF_2dbm(Cl)PLA	**13a**	7.5	466	6.91	520	113.6
	13b	18.7	437	2.57	516	168.0
BF_2dbm(Br)PLA	**14a**	6.4	471	5.32	522	28.9
	14b	17.1	436	1.79	520	47.1
BF_2dbm(I)PLA	**15a**	6.6	455	3.46	528	5.6
	15b	20.3	437	0.90	522	5.8

[a]Number-average molecular weight (GPC). [b]Steady-state fluorescence spectra emission maximum under air. Excitation source: 369 nm xenon lamp. [c]Fluorescence lifetime excited with a 369 nm light-emitting diode (LED) monitored at the emission maximum. All fluorescence lifetimes are fitted with triple-exponential decay. [d]Delayed emission spectra maxima under N_2. Excitation source: xenon flash lamp. [e]Pre-exponential weighted RTP lifetime. Excitation source: xenon flash lamp; RTP lifetime fit to triple-exponential decay.

Table 2. Optical Properties of Boron Dye Initiators and Polymers in CH_2Cl_2

sample		λ_{abs}[a] (nm)	ε[b] (M^{-1} cm^{-1})	λ_{em}[c] (nm)	τ_F[d] (ns)	Φ_F[e]
BF_2dbmOH	**6**	397	53 000	433	1.96[f]	0.95
BF_2dbmPLA	**11a**	396	52 000	425	1.94	0.95
BF_2dbm(F)OH	**7**	397	48 000	430	3.27	0.99
BF_2dbm(F)PLA	**12a**	397	45 000	426	1.95	0.98
BF_2dbm(Cl)OH	**8**	401	56 000	438	3.43	0.99
BF_2dbm(Cl)PLA	**13a**	398	55 000	435	1.96	0.99
BF_2dbm(Br)OH	**9**	403	56 000	440	2.24	0.96
BF_2dbm(Br)PLA	**14a**	404	54 000	438	1.77	0.91
BF_2dbm(I)OH	**10**	407	58 000	441	1.03[g]	0.55
BF_2dbm(I)PLA	**15a**	405	49 000	435	0.95	0.40

[a]Absorption maxima. [b]Extinction coefficients calculated at the absorption maxima. [c]Fluorescence emission maxima excited at 369 nm. [d]Fluorescence lifetime excited with a 369 nm light-emitting diode (LED) monitored at the emission maximum. All fluorescence lifetimes are fitted with single-exponential decay. [e]Relative quantum yield, versus anthracene in EtOH as a standard. [f]Values taken from ref 18. [g]Values taken from ref 22.

DOI: 10.1021/acsami.5b07126
ACS Appl. Mater. Interfaces 2015, 7, 23633–23643

Molecular weight is an effective way to tune the luminescence properties of boron dye-PLA materials.[19,20,22,23] In previously reported BF_2dbmPLA polymer conjugates, low MW polymers (~4 kDa) showed green fluorescence (500 nm), high MW polymers (~20 kDa) showed blue fluorescence (425 nm), and peak emission could be modulated using the PLA MW or dye concentration in blends.[19] This is attributed to a change in the dye−dye interactions within the PLA matrix; therefore, dye concentration plays an important role. Similarly, this concentration-dependent emission can also be seen in other difluoroboron dyes. For example, Venkatesan et al. successfully generated β-ketoiminates that exhibited phosphorescence across the visible spectrum at different concentrations in CH_2Cl_2 and poly(methyl methacrylate) (PMMA) environments.[11] In the solid-state, dye structure is critical in determining how dye−dye interactions influence material optical properties. Phenyl−phenyl systems (BF_2dbmPLA) reached a maximal blue-shifted fluorescence at a MW of ~20 kDa, which corresponded to ~1% dye by total mass; further dilution did not affect the fluorescence color significantly.[19] With increased conjugation in naphthyl−naphthyl-based dyes (BF_2dnmPLA), which corresponded to lower solubility and increased propensity for dyes to aggregate, a maximal blue-shifted fluorescence was reached with only 0.2% dye loading in PLA blends.[23]

Halide interactions play important roles in molecular assemblies and crystal engineering[22,45,46] and serve as a way to modulate optical properties. In this study, two polymers of each halide-substituted dye were prepared to analyze MW effects and dye−dye interactions on the optical properties. (See spectra of dye−polymer films in Figures S18−20 in the Supporting Information.) The expected trend in fluorescence lifetimes (τ_F) across the halide series is observed. As the halide becomes heavier, τ_F decreases (H = 6.6 ns, F = 45.4 ns, Cl = 6.9 ns, Br = 5.3 ns, I = 3.4 ns). The fluorescence color sensitivity to dye loading (i.e., M_n) also varied with different halide dyes. For instance, between BF_2dbm(F)PLA, **12a** (6.1 kDa; λ_F = 502 nm) and **12b** (16.5 kDa: λ_F = 428 nm), the emission wavelength shifted by 74 nm. In contrast, emission wavelengths for the bromide analogues BF_2dbm(Br)PLA, **14a** (6.0 kDa ; λ_F = 471 nm) and **14b** (17.1 kDa; λ_F = 436 nm), shifted only 35 nm with a comparable shift in molecular weight (see Figure 2 and Table 3). The difference in emission maxima between low MW and high MW polymers decreases for heavier halides. When heavy atoms are present, there is enhanced intersystem crossing (ISC) to the triplet state, siphoning off red-shifted fluorescence. The unsubstituted dye, BF_2dbmPLA, showed a smaller range than the chloro- and fluoro- adducts. This could be a result of increased inductive effects due to the electron-withdrawing properties of the aromatic halides influencing the donor−acceptor scaffold of the dye.[47−49] Fluorescence properties can inspire designs for future dye scaffolds, controlling color ranges within the PLA matrix and by modulating the donor−acceptor structure of the boron dyes.

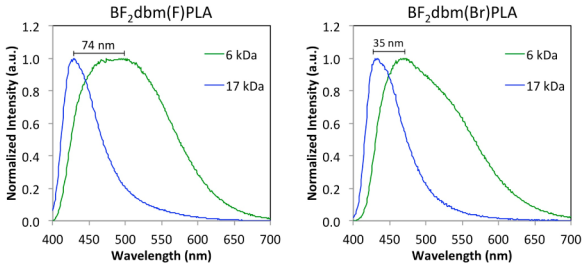

Figure 2. Molecular weight and fluorescence; total emission of BF_2dbm(F)PLA (**12**) and BF_2dbm(Br)PLA (**14**) in air (λ_{ex} = 369 nm).

The phosphorescence properties of boron polymers were studied under a N_2 atmosphere at room temperature. All polymers showed delayed emission in the absence of oxygen at room temperature (see Figure 3 and Figure S22 in the Supporting Information). Delayed emissions were green and the maxima ranged from 500 nm to 530 nm. Unlike the fluorescence maxima (λ_F), the phosphorescence maxima (λ_P) did not vary with polymer MW. For example, the fluorescence of BF_2dbmPLA (**11**) blue-shifted from 457 nm (~6 kDa) to 426 nm (~19 kDa), while the phosphorescence changed only slightly, from 516 nm to 510 nm with increasing MW. Heavier halide substituents red-shifted the phosphorescence (**11a−15a**; λ_P: H = 516 nm, F = 512 nm, Cl = 520 nm, Br = 522 nm, I = 528 nm). The emission peak also sharpened with heavier halide substituents, along with a decrease in delayed fluorescence at shorter wavelengths, similar to previously described BF_2bdk-PLA conjugates.[22] Because delayed fluorescence (DF) is temperature-sensitive, it is important to suppress DF in ratiometric oxygen probes, as the fluorescence internal "standard" would otherwise respond to O_2 quenching and temperature. The addition of heavier halides (Br and I) is an effective way to minimize the DF transitions.

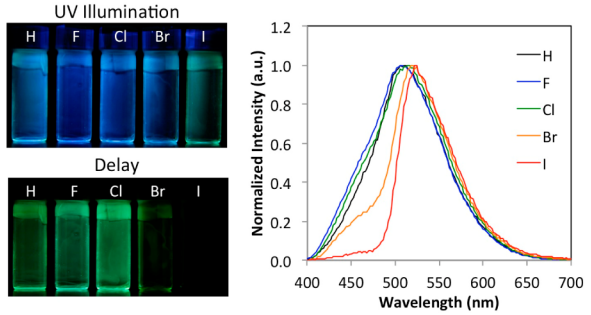

Figure 3. Phosphorescence of high MW BF_2dbm(X)PLA polymer films (**11b−15b**). (Left) Images of BF_2dbm(X)PLA films under N_2 with UV illumination and after the lamp is turned off (delay). (Right) Delayed emission spectra of films (excitation = xenon flash lamp with 2 ms delay).

The phosphorescence lifetime (τ_P) is highly dependent on both the molecular weight and the halide substituent. The phosphorescence emission maxima stayed at a constant wavelength with changing MW, while the fluorescence maxima blue-shifted. Increasing the molecular weight expanded the singlet−triplet gap, and decreased the rate of intersystem crossing and thermally activated delayed fluorescence, resulting in longer lifetimes (e.g., τ_P of BF_2dbmPLA: for **11a**, 142 ms; for **11b**, 207 ms). The halides influenced the τ_P differently. With increased atomic mass of the halide substituents, the phosphorescence intensity increased (Table 3), at the expense of the fluorescence intensity. Lighter halide substituents (H (**11a**), F (**12a**), and Cl (**13a**)) had weak phosphorescence shoulders in their total emission spectra under N_2 but long green afterglows (>100 ms lifetimes) (Figure 4). For heavier halide dyes (Br and I) with short polymers, the emission color of the material changed from blue-green (~470 nm) to yellow

DOI: 10.1021/acsami.5b07126
ACS Appl. Mater. Interfaces 2015, 7, 23633−23643

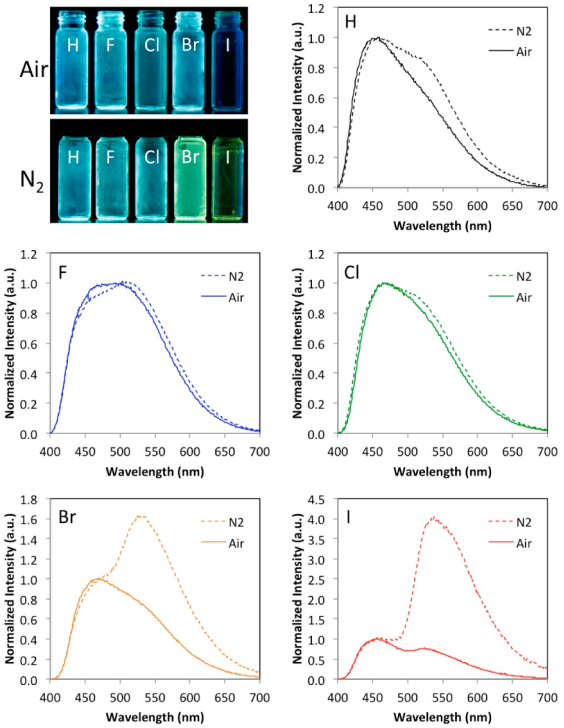

Figure 4. Images and total emission spectra of low MW polymer films (**11a**–**15a**) under air and nitrogen (λ_{ex} = 369 nm).

(~525 nm), as the phosphorescence dominated the total emission. These types of materials are well-suited for ratiometric sensing, where the fluorescence serves as the internal standard, and the phosphorescence intensity relates to the O_2 concentration. Lighter halide substituted dyes with long RTP lifetimes are well-suited for lifetime methods for quantifying O_2 concentration.

The fluorescence-to-phosphorescence intensity ratio (F/P) can be controlled by polymer MW.[22,23] This is linked to the singlet–triplet energy gap; as the gap becomes larger, the rate of ISC decreases, lowering the phosphorescence intensity. For short polymers, Br **14a** and I **15a**, the fluorescence and phosphorescence peaks overlap (Figure 4). Higher MW polymers can potentially resolve the two peaks to facilitate detection of the fluorescence and phosphorescence. This strategy has been demonstrated for naphthyl dye polymers to make them useful as ratiometric sensing materials.[23] For some naphthalene-substituted dyes, intense phosphorescence is still present, even for dilute dye samples (>20 kDa).[20,23] However, in other cases, as the singlet triplet energy gap gets larger, crossover to the triplet state and phosphorescence intensity are significantly decreased, rendering the material impractical for sensing. In fact, this is what is observed for bromine- and iodine-substituted BF_2dbm(X)PLA derivatives in this study. The singlet–triplet gap in 20 kDa polymers became so great that the phosphorescence no longer dominated the total emission under N_2 (see Figure S21 in the Supporting Information). The phosphorescence peak still resulted in a visible color change for BF_2dbm(I)PLA, but was much weaker than the fluorescence. Thus, while naphthyl dyes work well, even at low dye loading, BF_2dbm(X)PLA (X = Br, I) materials are most useful at higher dye loadings for ratiometric sensing.

Oxygen Sensitivity. The two most conventional ways for luminescence O_2 quantification are based on lifetime and intensity-based phosphorescence measurements. Lifetime methods do not require internal standards to determine O_2 concentration.[33] In this method, spectrally isolated fluorescence and phosphorescence peaks, or intense phosphorescence, are not needed for O_2 quantification, as long as the lifetime is gated and does not include the fluorescence.[33] Lifetime is directly linked to oxygen sensitivity, as shown in eqs 1 and 2.[50] Therefore, materials with the longest unquenched phosphorescence lifetimes (τ_0), and the fastest diffusion of oxygen through the matrix, will be the most sensitive. Klimant et al. recently developed ultrasensitive materials with aluminum or difluoroboron hydroxyphenalenone complexes within polystyrene, Teflon, and Hyflon polymer matrices.[51] By combining complexes of variable unquenched lifetimes, with polymer matrices of high O_2 permeabilities (P), such as polystyrene ($P \approx 8.8 \times 10^{-16}$ mol m^{-1} s^{-1} Pa^{-1}),[52] Hyflon ($P \approx 170 \times 10^{-16}$ mol m^{-1} s^{-1} Pa^{-1}),[53] or Teflon ($P \approx 1200 \times 10^{-16}$ mol m^{-1} s^{-1} Pa^{-1}),[54] the oxygen hypersensitivity could be tuned, and oxygen concentration could be detected in the parts per million range. In contrast, purely organic crystals exhibited long-lived phosphorescence, insensitive to oxygen. When the phosphorescence was confined to a crystal, the oxygen barrier was too great, and the phosphorescence persisted under ambient conditions.[29,30,55–58]

$$\frac{\tau}{\tau_0} = 1 + K_{SV}[O_2] \quad (1)$$

$$K_{SV} = \tau_0 k_D \quad (2)$$

This effect has yet to be studied for boron dyes in biodegradable polylactide. Polylactide exhibits permeabilities that are magnitudes lower than that of perfluorinated polymers and polystyrene (PLA: $P \approx 0.86 \times 10^{-16}$ mol m^{-1} s^{-1} Pa^{-1})[59] and can change, depending on material fabrication, film treatment (e.g., annealing), polymer microstructure (e.g., stereochemistry) and other factors that affect material microcrystallininty. At first, this might seem like a drawback, but, in fact, the lower permeability of oxygen in PLA is beneficial, given that it counterbalances the long-lived phosphorescence in BF_2bdkPLA materials. The net effect is biocompatible materials with dynamic ranges that are well-matched to biological processes. Another advantage of the long phosphorescence lifetimes in BF_2dbm(X)PLA materials is that they enable detection by convenient and inexpensive imaging techniques, such as that with portable high-speed cameras,[60] which can be useful in clinical and field contexts.

Given that phosphorescence lifetimes vary with halide substituent and polymer MW, samples **11**–**15** provide a convenient model to test O_2 sensitivity versus lifetime. Previously, it was shown that the phosphorescence intensity of BF_2dbm(I)PLA varied linearly with oxygen concentrations between 0% and 1%.[22] Highly sensitive dual-emitters within this O_2 range could assist in detecting tumors with severe hypoxia and be used in monitoring tumor growth and proliferation during therapy.[36] To determine sensitivity within this range, the unquenched phosphorescence lifetime (τ_0) (i.e., 0% oxygen) was compared to the lifetime at 1% oxygen (τ_1) (Table 4). The sensitivity of each polymer was determined by the rate of the change between the two O_2 concentrations (τ_0/τ_1), as is routine within the field for comparison between oxygen probes.[33]

Lighter halide substituted dye–polymer conjugates (H, F, and Cl) showed the most dynamic response to oxygen, as the

DOI: 10.1021/acsami.5b07126
ACS Appl. Mater. Interfaces 2015, 7, 23633–23643

Table 4. Lifetime Oxygen Sensitivity of BF_2dbm(X)PLA Films

sample		τ_0[a] (ms)	τ_1[b] (ms)	sensitivity[c]
BF_2dbmPLA	**11a**	142.1	10.2	13.9
	11b	207.4	14.7	14.1
BF_2dbm(F)PLA	**12a**	122.8	9.1	13.5
	12b	195.9	10.2	19.2
BF_2dbm(Cl)PLA	**13a**	113.6	7.7	14.7
	13b	168.0	9.7	17.3
BF_2dbm(Br)PLA	**14a**	28.9	5.8	5.0
	14b	47.1	6.9	6.8
BF_2dbm(I)PLA	**15a**	6.6	3.2	2.1
	15b	7.4	3.1	2.4

[a]Phosphorescence lifetime in N_2. [b]Phosphorescence lifetime in 1% O_2. [c]Sensitivity is defined as τ_0/τ_1.

phosphorescence lifetimes became ~14 times shorter at 1% oxygen. However, between these three samples, sensitivity changes are minimal (BF_2dbmPLA, **11a**, τ_0/τ_1 = 13.9; BF_2dbm(F)PLA, **12a**, τ_0/τ_1 = 13.5; BF_2dbm(Cl)PLA, **13a**, τ_0/τ_1 = 14.7). The sensitivities are too similar to conclude definitively that the lighter halides (F, Cl) are altering the oxygen sensitivity, as minor changes in polymer MW may be the defining factor for the observed changes (i.e., BF_2dbm(F)-PLA: **12a** (6.1 kDa) and BF_2dbm(Cl)PLA: **13a** (7.5 kDa)). At 1% oxygen, these dyes are approaching the upper limit of detection as well, defined as τ_1/τ_0 = 1% (e.g., BF_2dbmPLA: **11b**, τ_1/τ_0 = 7%).[61] Therefore, the detected phosphorescence at 1% oxygen may be the result of a different detectable solid-state species (i.e., aggregates or dimers) within the PLA matrix as BF_2dbm type fluorophores are well-known to form in polymer matrices.[62−64] Different phosphorescence quenching rates, or completely unquenchable species may also influence the sensitivity of these materials.[63] The mere presence of long-lived phosphorescence within the BF_2dbm(X)PLA samples, where X = H, F, and Cl, will indicate a highly deoxygenated environment, useful for numerous applications.[65]

The less dynamically sensitive bromine (**14**) and iodine (**15**) polymers serve as better systems for analyzing trends in phosphorescence lifetimes. The lifetimes of the bromide **14a** and iodide **15a** polymers under nitrogen were 28.9 and 6.6 ms, respectively. The resultant change in oxygen sensitivity was dramatic (Br, **14a**, τ_0/τ_1= 5.0; I, **15a**, τ_0/τ_1 = 2.1). In the higher MW polymers, **14b** and **15b**, τ_0 became longer, and thus, the sensitivity changed (Br, **14b**, τ_0/τ_1 = 6.8; I, **15b**, τ_0/τ_1 = 2.4). This suggests that heavy-atom substitution and polymer MW can effectively tune the oxygen sensitivity of these BF_2dbm-(X)PLA materials.

Oxygen-sensitive materials with the unique combination of millisecond long decays and intense phosphorescence are scarce.[22,51] Polymers with heavier-halide-substituted dyes, bromine (**14a**) and iodine (**15a** and **15b**), meet these criteria (Table 5). The long phosphorescence lifetimes can be used to detect oxygen by phosphorescence lifetime imaging microscopy (PLIM),[66] and the phosphorescence is strong enough for intensity-based ratiometric measurements.[22,23] When analyzing the fluorescence-to-phosphorescence (F/P) ratios of the low MW polymers, the bromide polymer (**14a**) experienced slightly

Table 5. Ratiometric Oxygen Sensitivity of BF_2dbm(X)PLA Films

sample	F/P_0[a]	F/P_1[b]	F/P_{21}[c]	sensitivity[d] (1% O_2)	sensitivity[e] (21% O_2)
14a	0.64	1.34	1.51	2.09	2.35
15a	0.28	0.45	1.15	1.61	4.10
15b	1.43	2.48	6.43	1.73	4.50

[a]Fluorescence/phosphorescence in N_2. [b]Fluorescence/phosphorescence in 1% O_2. [c]Fluorescence/phosphorescence in air (21% O_2). [d]$(F/P_1)/(F/P_0) = P_0/P_1$. [e]$P_0/P_{21}$.

higher sensitivity in the 0%−1% O_2 range than the iodide polymers (BF_2dbm(Br)PLA: **14a**, P_0/P_1 = 2.09, BF_2dbm(I)-PLA: **15a**, P_0/P_1 = 1.61) (Figure 5). More pronounced than

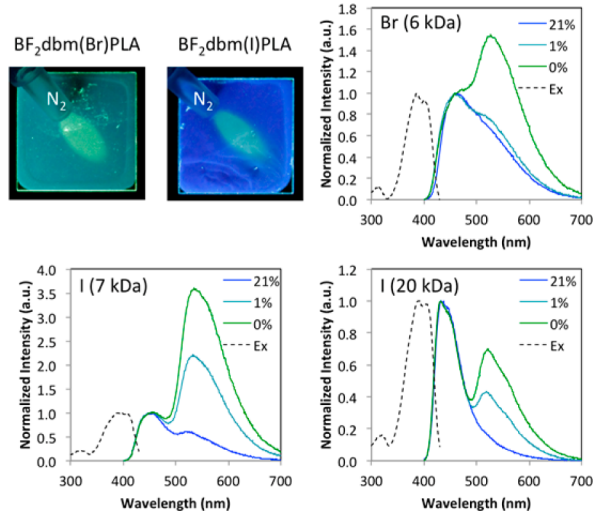

Figure 5. Oxygen-sensitive BF_2dbm(X)PLA polymers suitable for ratiometric sensing. Images show BF_2dbm(Br)PLA (**14a**, 6 kDa) and BF_2dbm(I)PLA (**15b**, 20 kDa) spin-cast films with a stream of nitrogen gas blown across the surface. Spectra represent excitation monitored at peak fluorescence wavelength (Ex, dashed line) and total emission spectra under 0% O_2 (nitrogen), 1% O_2 and 21% O_2 (air) (λ_{ex} = 369 nm).

sensitivity is the change in range and limits of detection with heavy-atom substitution. At 21% oxygen (air), the bromide polymer **14a** has a negligible difference in the F/P ratio, compared to the ratio at 1% (BF_2dbm(Br)PLA: **14a**, P_0/P_1 = 2.09, P_0/P_{21} = 2.35). In contrast, iodide polymers, **15a** and **15b**, have more intense phosphorescence that can sense well beyond 1% oxygen. Iodide polymers of different MWs have similar oxygen sensitivities, but the range of detection changes. The phosphorescence of high MW BF_2dbm(I)PLA (20 kDa) was fully quenched in air (21% O_2), whereas low MW BF_2dbm-(I)PLA (6 kDa) exhibited phosphorescence under ambient conditions (i.e., air). This suggests that oxygen levels higher than 21% could be detected with this sensing material. These results demonstrate that the oxygen sensing capability of BF_2dbm(X)PLA-type fluorophore probes can be fine-tuned with halide substitution and polymer molecular weight for a variety of applications in biological and other contexts.

Photostability. It is well-known that β-diketones can photobleach with UV exposure.[67] For example, in sunscreens, the diketone avobenzone is commonly used to absorb short-wave UVA radiation and is known to photodegrade over time.

DOI: 10.1021/acsami.5b07126
ACS Appl. Mater. Interfaces 2015, 7, 23633−23643

Recently, it was reported that halide substitution can create new degradation pathways for diketone compounds.[68] Furthermore, Zakharova and co-workers demonstrated that both boron detachment and singlet oxygen generation are relevant pathways for BF_2dbm degradation in organic solvents.[69] Thus, it is important to analyze the degradation and photobleaching of boron dye polymers to assess the material lifetime and accuracy for sensing.

Photostability studies were conducted by exposing spin-cast polymer films to UV light using a hand-held 4 W UV lamp (λ_{ex} = 369 nm) for 18 h. A monochrome camera was used to monitor the total intensity while the dyes were excited. An image was captured every 5 min during the 18 h period. This was a simple way to monitor multiple samples at once, and to eliminate environmental variations between samples. The resultant changes in intensity are shown in Figure 6. For

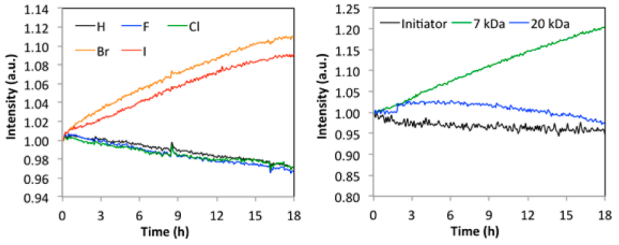

Figure 6. Influence of the halide substituent on the photostability of BF_2dbm(X)PLA spin-cast films. Total intensity versus UV exposure time (λ_{ex} = 369 nm; normalized to initial intensity). (Left) Short polymers **11a**–**15a**. (Right) Comparison of the photostability of **10** (initiator) and iodide polymers **15a** (7 kDa) and **15b** (20 kDa).

lighter-halide-substituted BF_2dbm(X)PLA (X = H, F, and Cl, **11a**–**13a**), the total intensity decreased, but only by ~5% over the 18 h period, which is consistent with only modest dye degradation. Compared to many fluorescent probes commonly used in biology,[1,2] these materials are intense and show excellent photostability. Furthermore, these findings confirm their suitability for lifetime oxygen sensing or as turn-on sensors in oxygen-free or very low oxygen environments.

Low MW polymers with bromide and iodide (**14a** and **15a**), in contrast, actually became 9%–10% brighter after excitation for 18 h (Figure 6). At first, it might seem surprising that the overall intensity increased, even though the number of fluorophores decreased upon photodegradation, but, in fact, this is understandable, given what is known about dye loading and ISC effects in BF_2bdkPLA materials.[22] When dye concentration decreases in PLA, the fluorescence blue-shifts and the energy gap between fluorescence and phosphorescence maxima increases. This decreases the rate of ISC to the oxygen-sensitive triplet state, which is quenched in air, and thus, results in more intense total emission. It is interesting to compare this process with mechanochromic luminescence quenching (MLQ) in solid BF_2bdk dye samples, wherein thermally annealed samples have a larger singlet triplet gap and are bright until smearing narrows the singlet triplet gap, thus facilitating ISC and quenching of the triplet state, causing the total emission to decrease.[32] Unlike the 7 kDa iodide polymer, the 20 kDa sample (**15b**) showed little change in the fluorescence maximum or total intensity over time (Figure 6). Given that the dye is already primarily in the monomeric state in the high MW polymer, it does not blue-shift upon photodegradation and further dilution. Higher MW samples show good photostability; however, some changes in the F/P intensity ratio are noted for phototreated 20 kDa BF_2dbm(I)-PLA analyzed under nitrogen (Figure 7, bottom right). It is

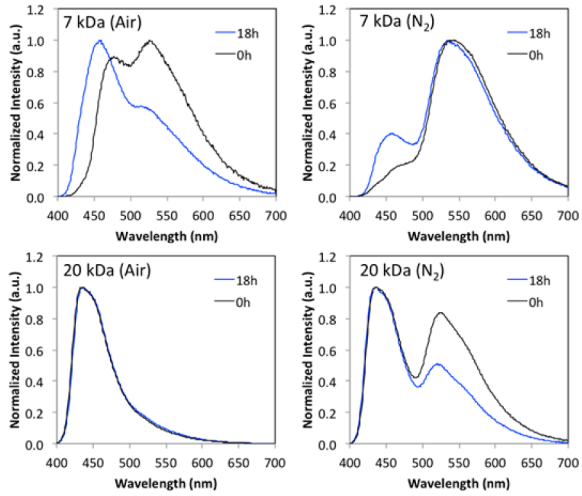

Figure 7. Total emission of BF_2dbm(I)PLA spin-cast films under air and nitrogen before (0 h) and after 18 h UV exposure in air (18 h) (λ_{ex} = 369 nm).

possible that dye monomers and aggregates could degrade at different rates in PLA samples. To test this, a control was run with initiator BF_2dbm(I)OH (**10**) spin-cast films. Results in Figure 6 (right) showed stable emission for this sample. In the solid state, however, under air or nitrogen, no phosphorescence is observed for **10**. This suggests involvement of the triplet state for photodegradation pathways through singlet oxygen generation or radical formation in dye-PLA films where phosphorescence is present. In summary, these findings indicate that high MW samples with long phosphorescence lifetimes (i.e., BF_2dbm(X)PLA where X = H, F, Cl) are best for lifetime imaging, given greater photostability. However, further improvements in dye design are required for reliable quantitative ratiometric sensing. Instead, heavy-atom-substituted dyes that exhibit strong phosphorescence at low dye loading are desirable.[20,23]

CONCLUSIONS

In summary, BF_2dbm(X)PLA materials were synthesized for X = H, F, Cl, Br, and I. The effects of changing the halide substituent, as well as the length of the PLA on the optical properties of the polymers, were studied in dilute CH_2Cl_2 solutions and solid-state films. All samples show intense fluorescence suitable for use as probes. Several properties ideal for oxygen sensing were also observed, including fluorescence and intense phosphorescence for the short iodine and bromine polymers suitable for ratiometric sensing, and long phosphorescence lifetimes for the lighter-halide-dye polymers useful for lifetime sensing and convenient and cost-effective camera imaging. The long lifetimes increased the sensitivity of the dye polymers. The lifetimes of the iodine and bromine polymers were shorter due to the heavy atom effect. Varying the polymer MW affected the fluorescence-to-phosphorescence (F/P) intensity ratio under anoxic conditions. For the long bromine and iodine polymers, increasing the polymer molecular weight (MW) to ~20 kDa created a larger singlet–triplet gap but decreased the rate of intersystem

DOI: 10.1021/acsami.5b07126
ACS Appl. Mater. Interfaces 2015, 7, 23633–23643

crossing (ISC). The result is slightly improved fluorescence and phosphorescence peak resolution but with much weaker phosphorescence, demonstrating that low MW BF_2dbm(X)-PLA polymers are preferable for ratiometric oxygen sensing.

Comparing the phosphorescence lifetimes of films under nitrogen versus a 1% oxygen environment revealed the ability to tune the oxygen sensitivity by changing the halide substituent from bromine to iodine or by changing the polymer MW. Finally, the photostability of the polymers was monitored over a continuous UV light excitation period of 18 h. The total intensity for the lighter halides decreased only 5% over time, indicating good photostability. Bromide and iodide derivatives, on the other hand, display an increase in fluorescence intensity, which counterintuitively, is also ascribed to dye degradation, and thus, lower dye loading. Dye dilution corresponds to a blue-shift in fluorescence, an increase in the singlet triplet energy gap, and thus, decreased rates of intersystem crossing, analogous to the molecular weight effect commonly observed for this family of materials.[21−23,25,26] The longer bromide- and iodide-substituted polymers did not show an increase in signal intensity upon extended exposure to UV light, given dyes existed in the maximally blue-shifted monomeric state both before and after UV illumination. Results from this investigation point to dyes with long lifetimes for lifetime imaging modalities or more-conjugated heavy-atom-substituted dyes with intense, separated, and readily detectable fluorescence and phosphorescence peaks for ratiometric sensing. And importantly, sensing materials should be made from high MW polymers (lower dye loading) to ensure photostability and reliable quantitative sensing with BF_2bdkPLA materials.

■ ASSOCIATED CONTENT

Supporting Information

The Supporting Information is available free of charge on the ACS Publications website at DOI: 10.1021/acsami.5b07126.

^{1}H NMR spectra of all new compounds, UV/vis spectra of boron complex initiators, fluorescence spectra of solution cast films in air, total emission of high molecular weight (MW) polymers in air and N_2, and delayed emission of low MW polymers (PDF)

■ AUTHOR INFORMATION

Corresponding Author

*E-mail: fraser@virginia.edu.

Author Contributions

The manuscript was written through contributions of all authors. All authors have given approval to the final version of the manuscript.

Notes

The authors declare no competing financial interest.

■ ACKNOWLEDGMENTS

We thank the National Institutes of Health (R01 CA167250) and UVA Cancer Center (to P30 CA44579) for support of this work. We gratefully acknowledge The Beckman Foundation for a Beckman Scholarship to C.K. We thank Dr. Gregory M. Palmer and Dr. Douglas Weitzel (Duke University) for helpful discussions.

■ REFERENCES

(1) Wolfbeis, O. An Overview of Nanoparticles Commonly Used in Fluorescent Bioimaging. *Chem. Soc. Rev.* **2015**, *44*, 4743−4768.

(2) Vollrath, A.; Schubert, S.; Schubert, U. S. Fluorescence Imaging of Cancer Tissue Based on Metal-Free Polymeric Nanoparticles−A Review. *J. Mater. Chem. B* **2013**, *1*, 1994−2007.

(3) Zheng, Q.; Juette, M. F.; Jockusch, S.; Wasserman, M. R.; Zhou, Z.; Altman, R. B.; Blanchard, S. C. Ultra-stable Organic Fluorophores for Single-molecule Research. *Chem. Soc. Rev.* **2014**, *43*, 1044−1056.

(4) Feng, Y.; Cheng, J.; Zhou, L.; Zhou, X.; Xiang, H. Ratiometric Optical Oxygen Sensing: A Review in Respect of Material Design. *Analyst* **2012**, *137*, 4885−4901.

(5) Yang, Y.; Zhao, Q.; Feng, W.; Li, F. Luminescent Chemodosimeters for Bioimaging. *Chem. Rev.* **2013**, *113*, 192−270.

(6) Loudet, A.; Burgess, K. BODIPY Dyes and their Derivatives: Syntheses and Spectroscopic Properties. *Chem. Rev.* **2007**, *107*, 4891−4932.

(7) Boens, N.; Leen, V.; Dehaen, W. Fluorescent Indicators Based on BODIPY. *Chem. Soc. Rev.* **2012**, *41*, 1130−1172.

(8) Ran, C.; Xu, X.; Raymond, S. B.; Ferrara, B. J.; Neal, K.; Bacskai, B. J.; Medarova, Z.; Moore, A. Design, Synthesis, and Testing of Difluoroboron-derivatized Curcumins as Near-infrared Probes for *In Vivo* Detection of Amyloid-β Deposits. *J. Am. Chem. Soc.* **2009**, *131*, 15257−15261.

(9) Yoshii, R.; Hirose, A.; Tanaka, K.; Chujo, Y. Functionalization of Boron Diiminates with Unique Optical Properties: Multicolor Tuning of Crystallization-Induced Emission and Introduction into the Main Chain of Conjugated Polymers. *J. Am. Chem. Soc.* **2014**, *136*, 18131−18139.

(10) Perumal, K.; Garg, J. A.; Blacque, O.; Saiganesh, R.; Kabilan, S.; Balasubramanian, K. K.; Venkatesan, K. β-Iminoenamine-BF_2 Complexes: Aggregation-Induced Emission and Pronounced Effects of Aliphatic Rings on Radiationless Deactivation. *Chem.—Asian J.* **2012**, *7*, 2670−2677.

(11) Koch, M.; Perumal, K.; Blacque, O.; Garg, J. A.; Saiganesh, R.; Kabilan, S.; Balasubramanian, K. K.; Venkatesan, K. Metal-Free Triplet Phosphors with High Emission Efficiency and High Tunability. *Angew. Chem.* **2014**, *126*, 6496−6500.

(12) Yoshii, R.; Tanaka, K.; Chujo, Y. Conjugated Polymers Based on Tautomeric Units: Regulation of Main-Chain Conjugation and Expression of Aggregation Induced Emission Property via Boron-Complexation. *Macromolecules* **2014**, *47*, 2268−2278.

(13) Sanchez, I.; Nunez, C.; Campo, J. A.; Torres, M. R.; Cano, M.; Lodeiro, C. Polycatenar Unsymmetrical β-diketonate Ligands as a Useful Tool to Induce Columnar Mesomorphism on Highly Luminescent Boron Difluoride Complexes. *J. Mater. Chem. C* **2014**, *2*, 9653−9665.

(14) Sanchez, I.; Mayoral, M. J.; Ovejero, P.; Campo, J. A.; Heras, J. V.; Cano, M.; Lodeiro, C. Luminescent Liquid Crystal Materials Based on Unsymmetrical Boron Difluoride β-Diketonate Adducts. *New J. Chem.* **2010**, *34*, 2937−2942.

(15) Xin, L.; Chen, Y. Z.; Niu, L. Y.; Wu, L. Z.; Tung, C. H.; Tong, Q.; Yang, Q. Z. A Selective Turn-on Fluorescent Probe for Cd^{2+} Based on a Boron Difluoride β-Dibenzoyl Dye and its Application in Living Cells. *Org. Biomol. Chem.* **2013**, *11*, 3014−3019.

(16) Zhang, G.; Lu, J.; Sabat, M.; Fraser, C. L. Polymorphism and Reversible Mechanochromic Luminescence for Solid-state Difluoroboron Avobenzone. *J. Am. Chem. Soc.* **2010**, *132*, 2160−2162.

(17) Galer, P.; Korosec, R. C.; Vidmar, M.; Sket, B. Crystal Structures and Emission Properties of the BF_2 Complex 1-Phenyl-3-(3, 5-dimethoxyphenyl)-propane-1, 3-dione: Multiple Chromisms, Aggregation-or Crystallization-Induced Emission, and the Self-Assembly Effect. *J. Am. Chem. Soc.* **2014**, *136*, 7383−7394.

(18) Zhang, G.; Chen, J.; Payne, S. J.; Kooi, S. M.; Demas, J. N.; Fraser, C. L. Multi-emissive Difluoroboron Dibenzoylmethane Polylactide Exhibiting Intense Fluorescence and Oxygen-Sensitive Room-Temperature Phosphorescence. *J. Am. Chem. Soc.* **2007**, *129*, 8942−8943.

(19) Zhang, G.; Kooi, S. E.; Demas, J. N.; Fraser, C. L. Emission Color Tuning with Polymer Molecular Weight for Difluoroboron Dibenzoylmethane-Polylactide. *Adv. Mater.* **2008**, *20*, 2099−2104.

DOI: 10.1021/acsami.5b07126
ACS Appl. Mater. Interfaces 2015, 7, 23633−23643

(20) Samonina-Kosicka, J.; DeRosa, C. A.; Morris, W. A.; Fan, Z.; Fraser, C. L. Dual-Emissive Difluoroboron Naphthyl-Phenyl β-Diketonate Polylactide Materials: Effects of Heavy Atom Placement and Polymer Molecular Weight. *Macromolecules* **2014**, *47*, 3736−3746.
(21) Samonina-Kosicka, J.; Weitzel, D. H.; Hofmann, C. L.; Hendargo, H.; Hanna, G.; Dewhirst, M. W.; Palmer, G. M.; Fraser, C. L. Luminescent Difluoroboron β-Diketonate PEG-PLA Oxygen Nanosensors for Tumor Imaging. *Macromol. Rapid Commun.* **2015**, *36*, 694−699.
(22) Zhang, G.; Palmer, G. M.; Dewhirst, M. W.; Fraser, C. L. A Dual-Emissive-Materials Design Concept Enables Tumour Hypoxia Imaging. *Nat. Mater.* **2009**, *8*, 747−751.
(23) DeRosa, C. A.; Samonina-Kosicka, J.; Fan, Z.; Hendargo, H. C.; Weitzel, D. H.; Palmer, G. M.; Fraser, C. L. Oxygen Sensing Difluoroboron Dinaphthoylmethane Polylactide. *Macromolecules* **2015**, *48*, 2967−2977.
(24) Oh, J. K. Polylactide (PLA)-Based Amphiphilic Block Copolymers: Synthesis, Self-Assembly, and Biomedical Applications. *Soft Matter* **2011**, *7*, 5096−5108.
(25) Tang, L.; Tong, R.; Coyle, V. J.; Yin, Q.; Pondenis, H.; Borst, L. B.; Cheng, J.; Fan, T. M. Targeting Tumor Vasculature with Aptamer-Functionalized Doxorubicin−Polylactide Nanoconjugates for Enhanced Cancer Therapy. *ACS Nano* **2015**, *9*, 5072−5081.
(26) Pfister, A.; Zhang, G.; Zareno, J.; Horwitz, A. F.; Fraser, C. L. Boron Polylactide Nanoparticles Exhibiting Fluorescence and Phosphorescence in Aqueous Medium. *ACS Nano* **2008**, *2*, 1252−1258.
(27) Bowers, D. T.; Tanes, M. L.; Das, A.; Lin, Y.; Keane, N. A.; Neal, R. A.; Ogle, M. E.; Brayman, K. L.; Fraser, C. L.; Botchwey, E. A. Spatiotemporal Oxygen Sensing Using Dual Emissive Boron Dye−Polylactide Nanofibers. *ACS Nano* **2014**, *8*, 12080−12091.
(28) Baranoff, E.; Curchod, B. F. E.; Monti, F.; Steimer, F.; Accorsi, G.; Tavernelli, I.; Rothlisberger, U.; Scopelliti, R.; Gratzel, M.; Nazeeruddin, M. K. Influence of Halogen Atoms on a Homologous Series of Bis-Cyclometalated Iridium(III) Complexes. *Inorg. Chem.* **2012**, *51*, 799−811.
(29) Bolton, O.; Lee, K.; Kim, H. J.; Lin, K. Y.; Kim, J. Activating Efficient Phosphorescence from Purely Organic Materials by Crystal Design. *Nat. Chem.* **2011**, *3*, 205−210.
(30) Bolton, O.; Lee, D.; Jung, J.; Kim, J. Tuning the Photophysical Properties of Metal-Free Room Temperature Organic Phosphors via Compositional Variations in Bromobenzaldehyde/Dibromobenzene Mixed Crystals. *Chem. Mater.* **2014**, *26*, 6644−6649.
(31) Yoshii, R.; Suenaga, K.; Tanaka, K.; Chujo, Y. Mechanofluorochromic Materials Based on Aggregation-Induced Emission-Active Boron Ketoiminates: Regulation of the Direction of the Emission Color Changes. *Chem.—Eur. J.* **2015**, *21*, 7231−7237.
(32) Morris, W. A.; Liu, T.; Fraser, C. L. Mechanochromic Luminescence of Halide-Substituted Difluoroboron β-Diketonate Dyes. *J. Mater. Chem. C* **2015**, *3*, 352−363.
(33) Wang, X-d.; Wolfbeis, O. Optical Methods for Sensing and Imaging Oxygen: Materials, Spectroscopies and Applications. *Chem. Soc. Rev.* **2014**, *43*, 3666−2761.
(34) Carreau, A.; Hafny-Rahbi, B. E.; Matejuk, A.; Grillon, C.; Kieda, C. Why is the Partial Oxygen Pressure of Human Tissues a Crucial Parameter? Small Molecules and Hypoxia. *J. Cell. Mol. Med.* **2011**, *15*, 1239−1253.
(35) Tredan, O.; Galmarini, C. M.; Patel, K.; Tannock, I. F. Drug Resistance and the Solid Tumor Microenvironment. *J. Natl. Cancer Inst.* **2007**, *99*, 1441−1454.
(36) Vaupel, P.; Kallinowski, F.; Okunieff, P. Blood Flow, Oxygen and Nutrient Supply, and Metabolic Microenvironment of Human Tumors: A Review. *Cancer Res.* **1989**, *49*, 6449−6465.
(37) Sinks, L. E.; Roussakis, E.; Esipova, T. V.; Vinogradov, S. A. Synthesis and Calibration of Phosphorescent Nanoprobes for Oxygen Imaging in Biological Systems. *J. Visualized Exp.* **2010**, *37*, 1731.
(38) Bender, J. L.; Corbin, P. S.; Fraser, C. L.; Metcalf, D. H.; Richardson, F. S.; Thomas, E. L.; Urbas, A. M. Site-Isolated Luminescent Europium Complexes with Polyester Macroligands: Metal-Centered Heteroarm Stars and Nanoscale Assemblies with Labile Block Junctions. *J. Am. Chem. Soc.* **2002**, *124*, 8526−8527.
(39) Williams, D. B. G.; Lawton, M. Drying of Organic Solvents: Quantitative Evaluation of the Efficiency of Several Desiccants. *J. Org. Chem.* **2010**, *75*, 8351−8354.
(40) Heller, C. A.; Henry, R. A.; Mclaughlin, B.; Bliss, D. E. J. Fluorescence Spectra and Quantum Yields. Quinine, Uranine, 9,10-Diphenylanthracene, and 9,10-bis(Phenylethynyl) anthracenes. *J. Chem. Eng. Data* **1974**, *19*, 214−219.
(41) Melhuish, W. H. Quantum Efficiencies of Fluorescence of Organic Substances: Effect of Solvent and Concentration of the Fluorescent Solute. *J. Phys. Chem.* **1961**, *65*, 229−235.
(42) Jiménez Rioboo, R. J.; Philipp, M.; Ramos, M. A.; Kruger, J. K. Concentration and Temperature Dependence of the Refractive Index of Ethanol−Water Mixtures: Influence of Intermolecular Interactions. *Eur. Phys. J. E: Soft Matter Biol. Phys.* **2009**, *30*, 19−26.
(43) Johnson, R. M.; Fraser, C. L. Metalloinitiation Routes to Biocompatible Poly(lactic acid) and Poly(acrylic acid) Stars with Luminescent Ruthenium Tris(bipyridine) Cores. *Biomacromolecules* **2004**, *5*, 580−588.
(44) Chen, J.; Gorczynski, J.; Zhang, G.; Fraser, C. L. Iron Tris(dibenzoylmethane-polylactide). *Macromolecules* **2010**, *43*, 4909−4920.
(45) Kwon, M. S.; Lee, D.; Seo, S.; Jung, J.; Kim, J. Tailoring Intermolecular Interactions for Efficient Room-Temperature Phosphorescence from Purely Organic Materials in Amorphous Polymer Matrices. *Angew. Chem., Int. Ed.* **2014**, *53*, 11177−11181.
(46) Priimagi, A.; Cavallo, G.; Metrangolo, P.; Resnati, G. The Halogen Bond in the Design of Functional Supramolecular Materials: Recent Advances. *Acc. Chem. Res.* **2013**, *46*, 2686−2695.
(47) Wang, D.; Kang, Y.; Fan, L.; Hu, Y.; Zheng, J. Synthesis and Photoluminescence Behavior of Difluoroboron Complexes with β-Diketone Ligands. *Opt. Mater.* **2013**, *36*, 357−361.
(48) Ono, K.; Yamaguchi, H.; Taga, K.; Saito, K.; Nishida, J.-i.; Yamashita, Y. Synthesis and Properties of BF_2 Complexes to Dihydroxydiones of Tetracene and Perylene: Novel Electron Acceptors Showing *n*-type Semiconducting Behavior. *Org. Lett.* **2009**, *11*, 149−152.
(49) Ono, K.; Hashizume, J.; Yamaguchi, H.; Tomura, M.; Nishida, J.; Yamashita, Y. Synthesis, Crystal Structure, and Electron-Accepting Property of the BF_2 Complex of a Dihydroxydione with a Perfluorotetracene Skeleton. *Org. Lett.* **2009**, *11*, 4326−4329.
(50) Lackowicz, J. R. *Principles of Fluorescence Spectroscopy*, 3rd Edition; Springer: New York, 2006.
(51) Lehner, P.; Staudinger, C.; Borisov, S. M.; Klimant, I. Ultrasensitive Optical Oxygen Sensors for Characterization of Nearly Anoxic Systems. *Nat. Commun.* **2014**, *5*, 4460.
(52) Brandrup, J.; Immergut, E. H.; Grulke, E. A. *Polymer Handbook*, 4th Edition; Wiley: New York, 2004.
(53) Arcella, V.; Ghielmi, A.; Tommasi, G. High Performance Perfluoropolymer Films and Membranes. *Ann. N. Y. Acad. Sci.* **2003**, *984*, 226−244.
(54) Nemser, S. M.; Roman, I. C. U.S. Patent 5 051 114, 1991.
(55) Kuno, S.; Akeno, H.; Ohtani, H.; Yuasa, H. Visible Room-Temperature Phosphorescence of Pure Organic Crystals via a Radical-ion-pair Mechanism. *Phys. Chem. Chem. Phys.* **2015**, *17*, 15989−15995.
(56) Gong, Y.; Zhao, L.; Peng, Q.; Fan, D.; Yuan, W. Z.; Zhang, Y.; Tang, B. Z. Crystallization-Induced Dual Emission from Metal-and Heavy Atom-free Aromatic Acids and Esters. *Chem. Sci.* **2015**, *6*, 4438−4444.
(57) An, Z.; Zheng, C.; Tao, Y.; Chen, R.; Shi, H.; Chen, T.; Wang, Z.; Li, H.; Deng, R.; Liu, X.; Huang, W. Stabilizing Triplet Excited States for Ultralong Organic Phosphorescence. *Nat. Mater.* **2015**, *14*, 685−690.
(58) Zhang, X.; Xie, T.; Cui, M.; Yang, L.; Sun, X.; Jiang, J.; Zhang, G. General Design Strategy for Aromatic Ketone-Based Single-Component Dual-Emissive Materials. *ACS Appl. Mater. Interfaces* **2014**, *6*, 2279−2284.

DOI: 10.1021/acsami.5b07126
ACS Appl. Mater. Interfaces 2015, 7, 23633−23643

(59) Colomines, G.; Ducruet, V.; Courgneau, C.; Guinault, A.; Domenek, S. Barrier Properties of Poly(lactic acid) and its Morphological Changes Induced by Aroma Compound Sorption. *Polym. Int.* **2010**, *59*, 818−826.
(60) Meier, R. J.; Fischer, L. H.; Wolfbeis, O. S.; Schäferling, M. Referenced Luminescent Sensing and Imaging with Digital Color Cameras: A Comparative Study. *Sens. Actuators, B* **2013**, *177*, 500−506.
(61) Kochmann, S.; Baleizao, C.; Berberan-Santos, M. N.; Wolfbeis, O. S. Sensing and Imaging of Oxygen with Parts Per Billion Limits of Detection and Based on the Quenching of the Delayed Fluorescence of $^{13}C_{70}$ Fullerene in Polymer Hosts. *Anal. Chem.* **2013**, *85*, 1300−1304.
(62) Payne, S. J.; Fiore, G. L.; Fraser, C. L.; Demas, J. N. Luminescence Oxygen Sensor Based on a Ruthenium(II) Star Polymer Complex. *Anal. Chem.* **2010**, *82*, 917−921.
(63) Carraway, E.; Demas, J.; DeGraff, B. Luminescence Quenching Mechanism for Microheterogeneous Systems. *Anal. Chem.* **1991**, *63*, 332−336.
(64) Li, X.; Liu, H.; Sun, X.; Bi, G.; Zhang, G. Highly Fluorescent Dye-Aggregate-Enhanced Energy-Transfer Nanoparticles for Neuronal Cell Imaging. *Adv. Opt. Mater.* **2013**, *1*, 549−553.
(65) Zheng, X.; Tang, H.; Xie, C.; Zhang, J.; Wu, W.; Jiang, X. Tracking Cancer Metastasis *In Vivo* by Using an Iridium-Based Hypoxia-Activated Optical Oxygen Nanosensor. *Angew. Chem., Int. Ed.* **2015**, *54*, 8094−8099.
(66) Baggaley, E.; Botchway, S. W.; Haycock, J. W.; Morris, H.; Sazanovich, I. V.; Williams, J. A. G.; Weinstein, J. A. Long-lived Metal Complexes Open Up Microsecond Lifetime Imaging Microscopy Under Multiphoton Excitation: from FLIM to PLIM and Beyond. *Chem. Sci.* **2014**, *5*, 879−886.
(67) Sayre, R. M.; Dowdy, J. C.; Gerwig, A. J.; Shields, W. J.; Lloyd, R. V. Unexpected Photolysis of the Sunscreen Octinoxate in the Presence of the Sunscreen Avobenzone. *Photochem. Photobiol.* **2005**, *81*, 452−456.
(68) Yamaji, M.; Suwa, Y.; Shimokawa, R.; Paris, C.; Miranda, M. A. Photochemical Reactions of Halogenated Aromatic 1,3-Diketones in Solution Studied by Steady State, One-and Two-color Laser Flash Photolyses. *Photochem. Photobiol. Sci.* **2015**, *14*, 1673−1684.
(69) Zakharova, G. V.; Chibisov, A. K.; Sazhnikov, V. A.; Kononevich, Y. N.; Muzafarov, A. M.; Alfimov, M. V. Photodegradation of Boron Difluoride Dibenzoylmethanate in Solutions. *High Energy Chem.* **2013**, *47*, 327−330.

DOI: 10.1021/acsami.5b07126
ACS Appl. Mater. Interfaces 2015, 7, 23633−23643